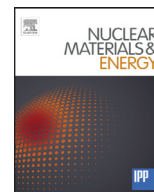




Contents lists available at ScienceDirect

Nuclear Materials and Energy

journal homepage: www.elsevier.com/locate/nme

Initial results of tests of depth markers as a surface diagnostic for fusion devices

L.A. Kesler^{a,b,*}, B.N. Sorbom^{a,b}, Z.S. Hartwig^b, H.S. Barnard^{a,b,c}, G.M. Wright^b, D.G. Whyte^{a,b}^a Department of Nuclear Science and Engineering, Massachusetts Institute of Technology, Cambridge, MA, 02139, USA^b Plasma Science and Fusion Center, Massachusetts Institute of Technology, Cambridge, MA, 02139, USA^c Lawrence Berkeley National Laboratory, 1 Cyclotron Road, Berkeley, CA 94720, USA

ARTICLE INFO

Article history:

Received 20 June 2016

Revised 23 October 2016

Accepted 12 November 2016

Available online 30 December 2016

Keywords:

Ion beam analysis

In situ diagnostic

AIMS

Depth marker

High-Z erosion

ABSTRACT

The Accelerator-Based In Situ Materials Surveillance (AIMS) diagnostic was developed to perform *in situ* ion beam analysis (IBA) on Alcator C-Mod in August 2012 to study divertor surfaces between shots. These results were limited to studying low-Z surface properties, because the Coulomb barrier precludes nuclear reactions between high-Z elements and the ~ 1 MeV AIMS deuteron beam. In order to measure the high-Z erosion, a technique using deuteron-induced gamma emission and a low-Z depth marker is being developed. To determine the depth of the marker while eliminating some uncertainty due to beam and detector parameters, the energy dependence of the ratio of two gamma yields produced from the same depth marker will be used to determine the ion beam energy loss in the surface, and thus the thickness of the high-Z surface. This paper presents the results of initial trials of using an implanted depth marker layer with a deuteron beam and the method of ratios. First tests of a lithium depth marker proved unsuccessful due to the production of conflicting gamma peaks, among other issues. However, successful trials with a boron depth marker show that it is possible to measure the depth of the marker layer with the method of gamma yield ratios.

© 2016 Published by Elsevier Ltd.

This is an open access article under the CC BY-NC-ND license.

<http://creativecommons.org/licenses/by-nc-nd/4.0/>

1. Introduction

¹The AIMS (Accelerator-based In situ Materials Surveillance) experiment, first implemented on Alcator C-Mod in August 2012, was designed to make *in situ* measurements of the inner divertor via ion beam analysis (IBA) [1]. While there are many surface diagnostics employed on tokamaks around the world, both *in situ* and *ex situ*, global and local, there still exist weaknesses in current diagnostic capabilities. Specifically, most *in situ* diagnostics have either limited spatial or time resolution, which prevents a complete understanding of the material transport properties within the tokamak [2]. The AIMS diagnostic was conceived to strengthen the current suite of surface diagnostics by using IBA to analyze various locations on the first wall, creating an *in situ* diagnostic that can be utilized between plasma discharges.

AIMS used a compact RFQ (radio frequency quadrupole) to produce a high-current, pulsed, 900 keV deuteron beam. This beam probed the inner divertor of Alcator C-Mod to perform *in situ* IBA. Between shots, the tokamak field coils were used to steer the beam to various locations of the divertor. By measuring the gamma and neutron spectra in AIMS, the ${}^2\text{H}(d,n){}^3\text{He}$ and ${}^{11}\text{B}(d,p\gamma){}^{12}\text{B}$ reactions were used to measure changes in both the retained deuterium fuel in the divertor [3], and the changes in the boron layer introduced during tokamak boronization [4].

While AIMS successfully measured low-Z elements of the plasma-facing components (PFCs) of the Alcator C-Mod divertor, it did not attempt to measure the erosion of the high-Z, bulk PFCs (i.e. tungsten, molybdenum, and the molybdenum alloy TZM). The Coulomb barrier between the deuterons and the high-Z target nuclei and the need for a reference to the surface make direct nuclear reaction analysis of the high-Z material impossible. A new technique is being developed to adapt AIMS to measure the high-Z erosion (and/or deposition) of the divertor and first wall, which enables analysis of all tokamak PFCs. The technique uses an implanted low-Z depth marker to both provide a target for

* Corresponding author.

E-mail address: kesler@mit.edu (L.A. Kesler).¹ AIMS = Accelerator-based In situ Materials Surveillance CLASS = Cambridge Laboratory for Accelerator-based Surface Science DANTE = Deuterium Accelerator-based Nuclear-reaction-producing Tandem Experiment.

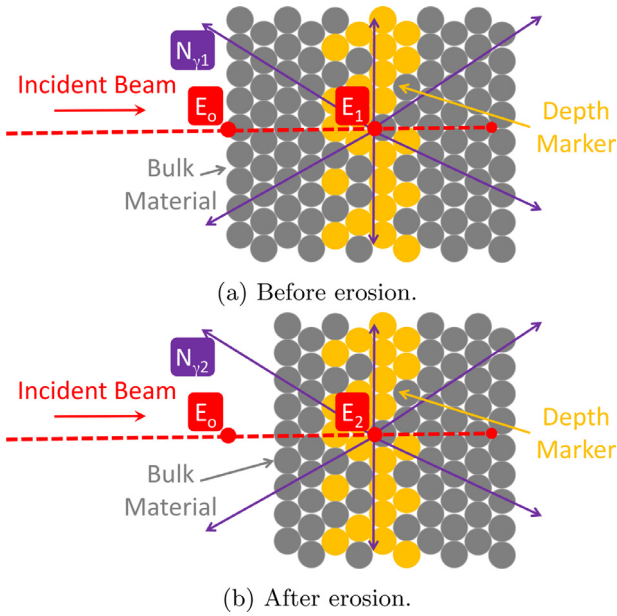


Fig. 1. As material is removed from the surface in (a), the incident deuterons pass through less material as shown in (b) and have a higher energy when reaching the depth marker. The cross section for gamma production increases with energy, leading to an increased in gamma yield. This increase (or decrease in the case of redeposition) in yield is the basis for AIMS erosion measurements.

the deuteron beam and to provide a reference to the surface with which to measure net erosion/deposition.

This work shows the successful implantation of a depth marker and the *ex situ* measurement of the depth of the layer with a deuteron beam. The successful result encourages the future study of depth markers as a potential surface diagnostic in a tokamak, including crosssection measurements and erosion studies.

2. Methods

Fig. 1 shows a schematic of how a depth marker would measure erosion or deposition. As the deuteron beam traverses the surface layer to the depth marker, it loses energy due to the stopping of charged ions in matter. Thus, the amount of high-Z material in the surface layer is directly related to the energy of the deuteron beam at the depth marker. The energy of the beam at the depth marker layer changes the differential cross section ($\frac{d\sigma}{d\Omega}$) for gamma production. The number of gammas produced is additionally dependent on the beam current (I), exposure time (t), thickness of the marker (d), density of the layer (n), efficiency of the detector (ϵ), and gamma transmission coefficient (τ). The constant, e , is the elementary charge. This leads to the relationship

$$Y_{\gamma} = \frac{d\sigma}{d\Omega}(E_D) \frac{It}{e} nd\epsilon\tau \quad (1)$$

where the number of gammas collected by the detector is, because of the energy dependence of the differential cross-section, dependent on the energy of the deuteron beam at the depth marker, and thus the thickness of the high-Z material on top of the marker. Multiple measurements over time would show the evolution of the high-Z layer as material is either removed or deposited.

While directly calculating the depth based on the yield of a single gamma-producing reaction would be possible, measuring the deuteron beam current in a tokamak is nontrivial. Additionally, the density and thickness of the marker layer would change over time, making the calculation less accurate. In order to reduce these sources of uncertainty, the ratio of the yields of two gammas pro-

duced from the same depth marker can be used,

$$\frac{Y_{\gamma 1}}{Y_{\gamma 2}} = \frac{\frac{d\sigma}{d\Omega_1}(E_D) \epsilon_1 \tau_1}{\frac{d\sigma}{d\Omega_2}(E_D) \epsilon_2 \tau_2} \quad (2)$$

which eliminates all parameters except the differential cross section, the transmission coefficient, and the detector efficiency, simplifying the calculation and reducing the sources of error. The transmission coefficient, the fraction of gammas which transmit through the material between the target and the detector, and the detector efficiency, the fraction of gammas incident on the detector that are absorbed by the detector, both depend on gamma energy and therefore are not equal for the two different gammas used in this measurement. These values can be determined with gamma sources and are not an impediment to the technique.

The differential cross section is the only factor that changes with deuteron energy as the beam interacts with the depth marker layer. Since the deuteron beam energy at the surface is well-known, finding the energy of the deuteron at the depth marker gives the energy change in the surface layer above the marker. The deuteron energy change is determined by the amount of material the beam passes through, or the thickness of the layer, and the type of material. The original AIMS technique, described by Hartwig et al. [3], can determine the low-Z impurities in a redeposited layer. Thus, the gamma yield ratio can produce a thickness measurement, and when multiple measurements are taken over time, changes due to erosion and redeposition of material can be determined.

The technique requires an implanted depth marker layer, created by the stopping of an incident, monoenergetic ion beam of the desired species. For the results presented here, the implantations were performed at the CLASS (Cambridge Laboratory for Accelerator-based Surface Science) facility with a 1.7 MV tandem accelerator. This accelerator is capable of producing beams of many species and charge states, allowing a range of isotopes and depths for the implanted layer. The implantation profile of the beam is determined using SRIM [5].

Once the implantation is completed, the sample is transferred to the target chamber of the DANTE (Deuterium Accelerator-based Nuclear-reaction-producing Tandem Experiment) accelerator. DANTE is a 1 MV tandem accelerator capable of producing H^+ and D^+ beams, and is located in a shielded research facility at the Massachusetts Institute of Technology (MIT) appropriate for remote monitoring of radiation-producing experiments. The production of D^+ beams requires radiation shielding because of the inherent neutron- and gamma-production from d-induced reactions.

The DANTE beam can be considered “AIMS-like” in that it can produce a high current deuteron beam for probing material surfaces *ex situ*. In this study, the beam will be used to probe the implanted target and produce d-induced gammas. This *ex situ* analysis will allow verification of the gamma ratio technique for depth markers that could be implemented *in situ* in a tokamak environment equipped with an AIMS or “AIMS-like” diagnostic.

Detectors with various scintillators, including HPGc, LaBr, and NaI, are used in combination with CAEN data acquisition electronics and the ADAQ framework [6], a suite of computational tools for data acquisition, control, and comprehensive offline analysis of detector data to record gamma spectra. Additional analysis was also done in the ROOT framework, which is the basis for the ADAQ software [7].

Because of the neutron and gamma production from deuteron reactions, the gamma spectra obtained from AIMS experiments are comprised of many background peaks. **Table 1** shows most of the background peaks that may be seen in AIMS experiments.

Table 1

Possible peaks in the spectra presented in this paper. Energies in bold represent gamma energies that are potential candidates for the depth marker technique [8,9,12].

| Gamma energy [MeV] | Nuclear Reaction |
|--------------------|---|
| 0.429 | ${}^6\text{Li}(d,n\gamma){}^7\text{Be}$ |
| 0.475 | ${}^{140}\text{Ce}(n,\gamma){}^{141}\text{Ce}$ |
| 0.478 | ${}^6\text{Li}(d,p\gamma){}^7\text{Li}$ |
| 0.511 | annihilation |
| 0.569 | ${}^{74}\text{Ge}(n,n'\gamma)$ |
| 0.585 | ${}^{27}\text{Al}(d,\alpha\gamma){}^{25}\text{Mg}$ |
| 0.596 | ${}^{73}\text{Ge}(n,\gamma)$ |
| | ${}^{74}\text{Ge}(n,n'\gamma)$ |
| 0.609 | ${}^{73}\text{Ge}(n,\gamma)$ |
| 0.656 | ${}^{19}\text{F}(d,p\gamma){}^{20}\text{F}$ |
| 0.662 | ${}^{140}\text{Ce}(n,\gamma){}^{141}\text{Ce}$ |
| 0.693 | ${}^{72}\text{Ge}(n,n'\gamma)$ |
| 0.823 | ${}^{19}\text{F}(d,p\gamma){}^{20}\text{F}$ |
| 0.847 | ${}^{56}\text{Fe}(n,n'\gamma)$ |
| 0.871 | ${}^{16}\text{O}(d,p\gamma){}^{17}\text{O}$ |
| | ${}^{19}\text{F}(d,\alpha\gamma){}^{17}\text{O}$ |
| 0.953 | ${}^{11}\text{B}(d,p\gamma){}^{12}\text{B}$ |
| 0.975 | ${}^{27}\text{Al}(d,\alpha\gamma){}^{25}\text{Mg}$ |
| 0.983 | ${}^{19}\text{F}(d,p\gamma){}^{20}\text{F}$ |
| | ${}^{27}\text{Al}(d,p\gamma){}^{28}\text{Al}$ |
| 1.014 | ${}^{27}\text{Al}(d,p\gamma){}^{28}\text{Al}$ |
| 1.057 | ${}^{19}\text{F}(d,p\gamma){}^{20}\text{F}$ |
| 1.238 | ${}^{56}\text{Fe}(n,n'\gamma)$ |
| 1.309 | ${}^{19}\text{F}(d,p\gamma){}^{20}\text{F}$ |
| 1.388 | ${}^{19}\text{F}(d,p\gamma){}^{20}\text{F}$ |
| 1.461 | ${}^{40}\text{K} \rightarrow \gamma + {}^{40}\text{Ar}$ |
| 1.634 | ${}^{19}\text{F}(d,n\gamma){}^{20}\text{Ne}$ |
| | ${}^{20}\text{F} \rightarrow {}^{20}\text{Ne} + \beta^- + \gamma$ |
| 1.674 | ${}^{11}\text{B}(d,p\gamma){}^{12}\text{B}$ |

3. Results

This initial study explored the literature for isotopes that would be appropriate depth marker options. Two of these isotopes were tested as depth markers in TZM and tungsten.

3.1. Depth marker material choice

The material used for the depth marker layer has several requirements. It must be nonintrinsic to the tokamak environment, eliminating many common isotopes, such as ${}^{12}\text{C}$ and ${}^{16}\text{O}$. This could also require tailoring to the specific device on which this technique would be implemented; beryllium, for example, would not work well in ITER or JET if the walls are beryllium-coated. Additionally, there must be two deuteron-induced gamma reactions with the marker, with a sufficiently large cross section as to produce peaks larger than the background gamma spectrum. These gammas must have a monotonic yield ratio with respect to energy in the energy regime where the deuteron beam will interact with the depth marker.

Sziki et al. [8] and Elekes et al. [9] give many of the possible reactions of deuterons with natural isotopes of elements with $Z < 20$. ${}^6\text{Li}$ has two peaks at 429 and 478 keV, as shown in Fig. 2. Additionally, ${}^{11}\text{B}$ has two peaks at 953 keV and 1674 keV. Since boronization is used in many tokamaks (including Alcator C-Mod), ${}^6\text{Li}$ was the first isotope investigated.

3.2. ${}^6\text{Li}$ tests

For the initial test of the depth marker concept, ${}^6\text{Li}$ was implanted with the CLASS accelerator at an energy of 1.2 MeV in TZM (Mo-0.50Ti-0.08Zr-0.02C), corresponding to a depth of 1.4 μm . After exposing the target to a 1.2 MeV deuterium beam, no gamma

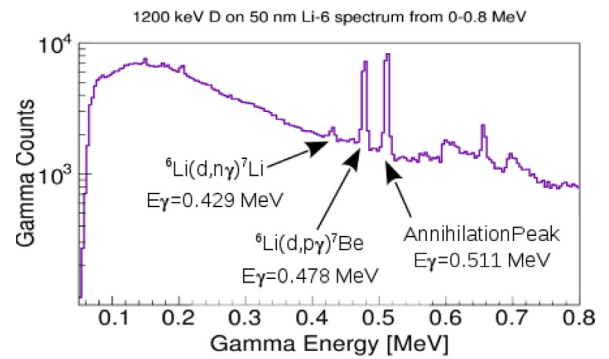


Fig. 2. Calibrated ${}^6\text{Li}$ spectrum taken at 135° off the beam axis. Note the proximity of the 511 keV annihilation peak.

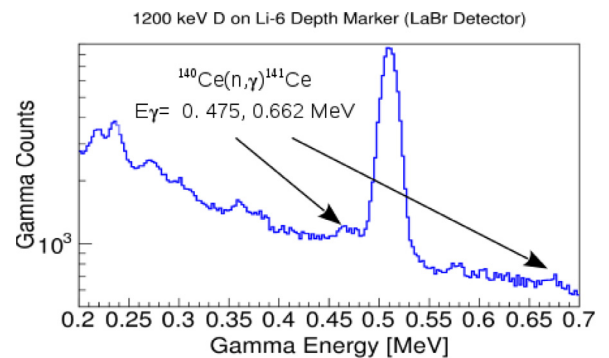


Fig. 3. Gamma spectrum on LaBr detector showing the n-induced peaks which interfere with detecting the 478 keV lithium peak.

peaks above background were seen on the spectrum collected with an HPGe detector. It is possible the layer diffused through the material due to the high diffusion coefficient of lithium in molybdenum [10]. Such diffusion would reduce the concentration of lithium in the marker layer, making the gamma production rate too low to resolve peaks above the background spectrum.

To avoid this issue, ${}^6\text{Li}$ was implanted in tungsten, in which it has a much lower mobility [11]. Results were still difficult to discern, for multiple reasons. First, the robust scintillator used in the AIMS experiment, LaBr, contains a cerium dopant. A neutron capture reaction, ${}^{140}\text{Ce}(n,\gamma){}^{141}\text{Ce}$ [12], produces multiple gamma energies, including one at 475 keV, as seen in Fig. 3. This peak would obscure the 478 keV d-induced peak from ${}^6\text{Li}$. Second, when using an HPGe detector to eliminate the cerium peak, the background induced from the Compton scattering of the 511 keV annihilation gammas is too large to discern the signal produced by the depth marker.

Because of these detector features, ${}^6\text{Li}$ is not suitable as an AIMS depth marker. The diffusivity in Mo is a concern for use in tokamaks with TZM PFCs, as is the interference from the Compton-scattered 511 keV annihilation gammas. Finally, the presence of a conflicting peak in the LaBr detector absolutely disqualifies the use of ${}^6\text{Li}$ as a depth marker in AIMS.

3.3. ${}^{11}\text{B}$ tests

The next isotope considered was ${}^{11}\text{B}$. While it could not be used in a boronized tokamak as a depth marker because of the interference from deuteron-induced gammas from the boronization layer with depth marker gammas, it would be a possibility in devices with an ITER-like wall. Boron diffusivity in pure tungsten is not known, but future studies will allow the determination of the stability of the depth marker. Sziki et al. [8] measured two prominent

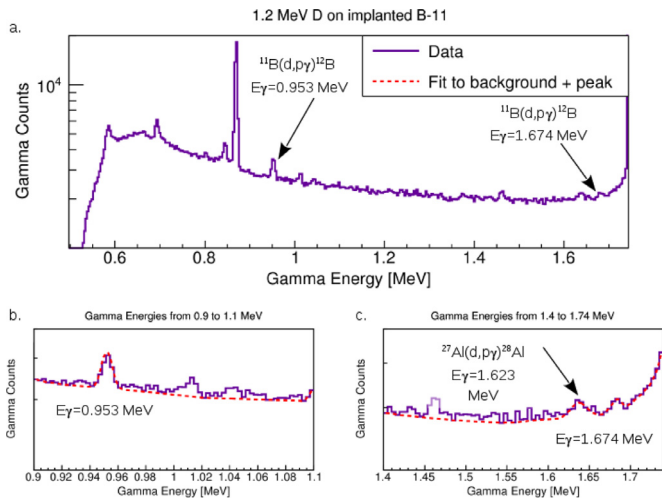


Fig. 4. Spectrum from deuteron beam on ^{11}B depth marker, taken on an HPGe detector. a. The full spectrum. b. The 0.953 MeV peak, with the background continuum and Gaussian peak fitted using ROOT. c. The 1.674 MeV peak, along with a neighboring background peak, with the background continuum and both Gaussian peaks fitted.

gamma production cross sections from boron, at an angle of 60° from the beam axis, for 850–2000 keV deuterons.

Boron was implanted in the target with the CLASS accelerator. A 2 MeV beam was used to implant ^{11}B at a range of $1.14\ \mu\text{m}$. After implantation, the sample was transferred to the DANTE accelerator and exposed to a 1.2 MeV deuteron beam. Fig. 4 shows the HPGe spectrum from this experiment.

Unlike the ^6Li spectra, two peaks are clearly present above background. While there are nearby peaks, none conflict with the signals from B^{11} within the HPGe detector resolution.

Fig. 5 shows the results from the depth marker measurements. The ratio (Eq. 2) obtained from the gamma yields is used to find

the energy of the deuteron beam at the depth marker by interpolating between points in the ratio of the cross sections from Sziki et al. [8]. SRIM range data is then used to calculate the depth of the layer based on the energy lost. The error is calculated for the ratio, and then the same calculations are performed on the upper and lower limits for the ratio to find the error in the depth measurement.

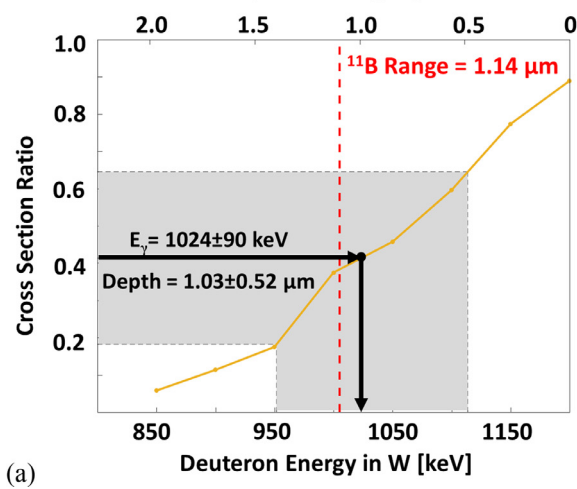
Background subtraction and integration of the peaks produces yields $Y_{953} = 3755.41 \pm 223.829$ and $Y_{1674} = 1096.76 \pm 230.647$. This gives a gamma yield ratio of $N_{1674}/N_{953} = 0.41 \pm 0.23$, taking into account detector efficiency and transmission. This gives a depth of $0.90\ \mu\text{m}$, with error defined by a lower limit of $0.51\ \mu\text{m}$ and an upper limit of $1.43\ \mu\text{m}$. This puts the known location of the layer from SRIM, $1.14\ \mu\text{m}$, within the error bars of this measurement. This result uses the range from SRIM, but a full calculation taking into account the straggle from the implantation peak should move the measured depth closer to the implantation depth.

4. Conclusions

The first *ex situ* test of a depth marker using gamma yield ratios successfully measured the location of an implanted marker. The test showed that ^{11}B is a possible isotope choice for the marker and that the technique can detect the location of an implanted layer within experimental error.

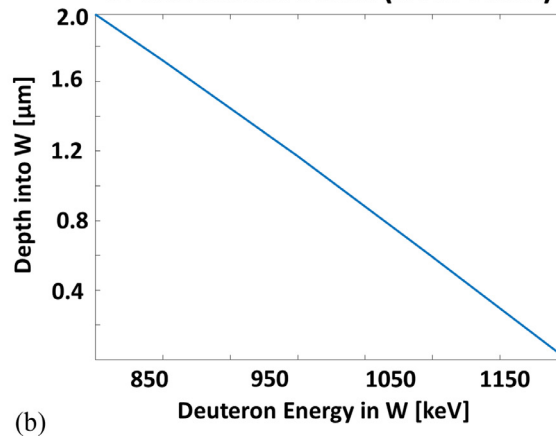
The experimental error at present is unacceptable for a diagnostic measuring *in situ* changes in the PFCs of a tokamak. Erosion rates in ASDEX-U and JET have been measured from 0.03 to $0.10\ \text{nm/s}$ [13]. In order to measure real time erosion rates in an operating long pulse tokamak, the resolution of the technique must be at least 100 nm. However, the error is mainly due to limitations of the experimental apparatus. Beam time was limited by the heating constraints of insulating sample mounts, and boron concentration was limited by access to the implantation beam. By reaching a higher concentration of boron in the surface and exposing the sample to the deuteron beam for longer intervals (or achieving higher deuteron beam current), the significant error in

Yield ratio as a function of depth and deuteron energy as it reaches the depth marker layer



(a)

Depth into W based on energy of deuteron beam (from SRIM)



(b)

Fig. 5. (a) The ratio of gamma yields leads to a determination of deuteron beam energy at the marker (lower x-axis), then calculation of depth marker (upper x-axis). The red dashed line marks the range of the marker as determined in SRIM [13], and the grayed area marks the error in the measurement. Cross section data is from Sziki et al. [8]. (b) The depth of the marker as a function of deuteron energy at the layer, calculated from SRIM [13], showing how the upper x-axis of (a) was determined. Note that the relationship between energy and depth appears linear, but is a function of the stopping power of deuterons in tungsten. (For interpretation of the references to colour in this figure legend, the reader is referred to the web version of this article.)

the yield integrals will be improved. The error additionally could be reduced with more accurate efficiency and transmission curves for the system and by increasing the counts under the peaks with longer exposure and better detector shielding.

These results successfully demonstrate that depth markers can be used to measure surfaces via ion beam analysis. In order to be implemented on a tokamak, error must be reduced to increase the resolution of the technique. In addition to decreasing error, next steps for this project include verification of the marker location with established techniques, studying the stability of the depth marker under high heat flux conditions (similar to an ITER-like divertor), and testing the system after performing *ex situ* erosion. Further refining of the technique will include measuring cross sections with greater energy and angular resolution, and identifying and measuring cross sections for other isotopes that may prove suitable for use as isotopic marker layers, such as ^{13}C .

This work is supported by the U.S. Department of Energy [grant number DE-FG02-94ER54235, cooperative agreement number DE-FC02-99ER54512].

References

- [1] Z. Hartwig, et al., An in situ accelerator-based diagnostic for plasma-material interactions science on magnetic fusion devices., *Rev. Sci. Instr.* 84 (2013). <http://dx.doi.org/10.1063/1.4832420>.
- [2] G. Federici, et al., Plasma-material interactions in current tokamaks and their implications for next step fusion reactors, *Nucl. Fusion* 41 (12) (2001) 1967.
- [3] Z.S. Hartwig, et al., Fuel retention measurements in Alcator C-Mod using accelerator-based in situ materials surveillance, *J. Nucl. Mater.* 463 (2015) 73–77. 21st International Conference on Plasma-Surface Interactions in Controlled Fusion Devices. <http://dx.doi.org/10.1016/j.jnucmat.2014.09.056>.
- [4] H. Barnard, Development of Accelerator Based Spatially Resolved Ion Beam Analysis Techniques for the Study of Plasma Materials Interactions in Magnetic Fusion Devices, Massachusetts Institute of Technology, 2014 Ph.D. thesis. <http://hdl.handle.net/1721.1/87495>.
- [5] J.F. Ziegler, et al., SRIM the stopping and range of ions in matter (2010), *Nucl. Instr. Methods Phys. Res. B* 268 (11–12) (2010) 1818–1823. 19th International Conference on Ion Beam Analysis. <http://dx.doi.org/10.1016/j.nimb.2010.02.091>
- [6] Z.S. Hartwig, The ADAQ framework: an integrated toolkit for data acquisition and analysis with real and simulated radiation detectors, *Nucl. Instr. Methods Phys. Res. A* 815 (2016) 42–49. <http://dx.doi.org/10.1016/j.nima.2016.01.017>.
- [7] R. Brun, F. Rademakers, Root an object oriented data analysis framework, *Nucl. Instrum. Methods Phys. Res. Sect. A* 389 (1) (1997) 81–86. [http://dx.doi.org/10.1016/S0168-9002\(97\)00048-X](http://dx.doi.org/10.1016/S0168-9002(97)00048-X).
- [8] G. Sziki, et al., Gamma ray production cross-sections of deuterium induced nuclear reactions for light element analysis, *Nucl. Instr. Methods Phys. Res. B* 251 (2) (2006) 343–351. <http://dx.doi.org/10.1016/j.nimb.2006.07.008>.
- [9] Z. Elekes, et al., Thick target γ -ray yields for light elements measured in the deuteron energy interval of 0.734 MeV, *Nucl. Instr. Methods Phys. Res. B* 168 (3) (2000) 305–320. [http://dx.doi.org/10.1016/S0168-583X\(99\)01003-4](http://dx.doi.org/10.1016/S0168-583X(99)01003-4).
- [10] C. Wu, The diffusion of lithium in molybdenum, *J. Chem. Phys.* 62 (12) (1975). <http://dx.doi.org/10.1063/1.430431>.
- [11] G. McCracken, H. Love, Diffusion of lithium through tungsten, *Phys. Rev. Lett.* 5 (5) (1960). <http://dx.doi.org/10.1103/PhysRevLett.5.201>.
- [12] J. Tuli, D. Winchell, Nuclear data sheets for A = 141, *Nucl. Data Sheets* 92 (2) (2001) 277–428. <http://dx.doi.org/10.1006/ndsh.2001.0004>.
- [13] M. Mayer, V. Rohde, G. Ramos, E. Vainonen-Ahlgren, J. Likonen, J.L. Chen, Erosion of tungsten and carbon markers in the outer divertor of asdex-upgrade, *Phys. Scr.* 2007 (T128) (2007) 106.